IEEE Access
Multidisciplinary ⋮ Rapid Review ⋮ Open Access Journal

Received 8 October 2023, accepted 8 December 2023, date of publication 12 December 2023,
date of current version 19 December 2023.

Digital Object Identifier 10.1109/ACCESS.2023.3342046

RESEARCH ARTICLE

A-MAD: An Adaptive-Microseismic Activity Detector Based on Gaussian Mixture Models and Spectral Subtraction

KAREN ROSERO[1], (Graduate Student Member, IEEE), CARLA PARRA[2], FELIPE GRIJALVA[3], (Senior Member, IEEE), JULIO CÉSAR LARCO[4], (Member, IEEE), ROMÁN LARA-CUEVA[4], (Senior Member, IEEE), AND NATHALY OROZCO GARZÓN[5], (Senior Member, IEEE)

[1]Department of Electrical and Computer Engineering, The University of Texas at Dallas, Richardson, TX 75080, USA
[2]Department of Signal Theory and Communications, Telematics and Computing Systems, Rey Juan Carlos University, Fuenlabrada, 28943 Madrid, Spain
[3]Colegio de Ciencias e Ingenierías "El Politécnico," Universidad San Francisco de Quito (USFQ), Quito 170901, Ecuador
[4]Departamento de Eléctrica, Electrónica y Telecomunicaciones, Universidad de las Fuerzas Armadas (ESPE), Sangolquí 171103, Ecuador
[5]Faculty of Engineering and Applied Sciences (FICA), Department of Telecommunications Engineering, Universidad de Las Américas (UDLA), Quito 170503, Ecuador

Corresponding author: Karen Rosero (kgr220000@utdallas.edu)

This work was supported in part by Universidad de Las Américas (UDLA), Ecuador, through the Research Project, under Grant ERT.NOG.23.13.01; in part by Universidad San Francisco de Quito (USFQ) through the Poli-Grants Program under Grant 17993; and in part by Universidad de las Fuerzas Armadas (ESPE) under Grant 2016-EXT-038.

ABSTRACT Continuous monitoring of active volcanoes is essential for understanding their behavior and providing accurate forecasts and warnings. Automating the detection of volcano microseismic events plays a crucial role in large-scale analysis, early warning systems, and efficient handling of large-scale data. This paper presents a novel approach for the automated detection of microseismic events associated with volcanic activity, focusing on the Cotopaxi volcano in Ecuador. Inspired by voice activity detection (VAD) systems used in speech processing, we propose an Adaptive-Microseismic Activity Detector (A-MAD) that modifies VAD techniques to identify frames within seismic signals containing volcanic activity. The A-MAD system incorporates a spectral subtraction stage to mitigate the impact of environmental noise and employs Gaussian Mixture Models (GMMs) to model the probabilistic distribution of microseismic events. Mel Frequency Cepstral Coefficients (MFCCs) are used as features to describe the seismic signals, enabling adaptability for varying noise levels. Experimental results on signals from Cotopaxi Volcano in Ecuador demonstrate the effectiveness of the A-MAD system, achieving high accuracy (96.39% for discrete events and 98.45% for continuous signals) while meeting the efficiency requirements of volcano monitoring institutions. This work contributes to the advancement of early warning systems for volcanic eruptions, providing a robust and adaptive approach for microseismic activity detection.

INDEX TERMS Volcanic seismic events, Gaussian mixture models, volcano monitoring.

I. INTRODUCTION

A. MOTIVATION

Natural disasters are inherently unpredictable, making it crucial to provide sufficient information based on scientific understanding to support early warning systems [1]. Volcanic eruptions unleash various detrimental effects on nearby populations, including gas emissions, ashfall, lahars on the volcano's flanks, and lava flows. Continuous monitoring of active volcanoes helps experts provide accurate forecasts and warnings, which reduces the risks faced by nearby communities [2]. Scientists analyze the characteristics and patterns of the monitored seismic signals to assess the likelihood of an eruption [3], [4]. Specifically, we focus

The associate editor coordinating the review of this manuscript and approving it for publication was Manuel Rosa-Zurera.

on *microseismic* events, also known as *micro-earthquakes*, to assess potential volcanic eruptions.

In Ecuador, the responsibility for monitoring seismic and volcanic activity lies with the ''Instituto Geofísico de la Escuela Politécnica Nacional'' (IGEPN), which duly notifies the competent authorities in the event of a necessary warning alert. The Cotopaxi volcano, located in north-central Ecuador, is closely monitored by the IGEPN since its eruption and subsequent generation of lahars can endanger the population living close to the main fluvial drainages [5]. Therefore, this research focuses on the analysis of the microseismic events found in the seismic signals of the Cotopaxi volcano.

The IGEPN observatory used to rely on visual methods to detect and classify microseismic events, which may introduce human errors due to the overwhelming volume of data to analyze daily [6], [7]. Currently, the detection stage is performed by using a micro-earthquake detector of Short-Term Average/Long-Term Average (STA/LTA) [8], which reaches an accuracy of 90% for detecting microseismic events. However, the effectiveness of the STA/LTA method depends on the SNR of the seismic signal. Then, if the background noise in the signal increases, the system can lead to false detections.

Further works on the detection of microseismic events adapted Voice Activity Detection (VAD) systems for seismic signals. The real-time detector presented in [6] improved the detection of microseismic events associated with volcanic activity. However, the system hardly relies on a handpicked minimum energy threshold. This manual parameter selection has two disadvantages: it would not be efficient if the SNR of the seismic signal changes, and its adaptation for seismic signals of a different volcano would be a cumbersome task. Therefore, there is a need to develop a system with robust performance under noisy conditions, and whose efficiency does not require manual selection of parameters.

B. CONTRIBUTIONS

In this work, we adapt VAD algorithms that identify speech segments within an utterance to identify frames within a seismic signal that contain microseismic volcanic activity. We refer to these systems as Microseismic Activity Detectors (MAD).

Environmental conditions primarily introduce irrelevant information into seismic signals, which can hinder the early detection of eruption events. Considering the limitations of energy-based MAD systems in handling additive noise within the signal, incorporating a signal enhancement stage becomes crucial to prevent segments without seismic activity from being misclassified as micro-earthquakes. This signal enhancement technique, which has been widely used in VAD systems, is the focus of our investigation. We aim to demonstrate its relevance in the context of seismic volcanic signals, where the Signal-to-Noise Ratio (SNR) may vary, even within signals recorded by the same station. Thus, we implement a spectral subtraction stage that mitigates the impact of environmental noise for improved microseismic activity detection. Furthermore, adopting a probabilistic modeling approach that learns the probability distribution for each class (segments with or without microseismic activity) provides a more robust representation of the energy distribution compared to simple threshold-based methods for class determination. Selecting appropriate features to describe the seismic signal is another area of exploration in microseismic event detection, as it has been proven to enhance detection performance [9].

In this context, our paper introduces A-MAD, an Adaptive-Microseismic Activity Detector that extracts characteristics from each individual utterance, allowing the system to adapt to varying noise levels in different seismic signals. Concretely, our contributions are:

i) Unlike traditional methods that rely solely on an energy threshold, we propose a technique that utilizes Gaussian Mixture Models (GMMs) to model the probability distribution of microseismic event occurrences.

ii) We incorporate a spectral subtraction stage to enhance the SNR, enabling robust detection even in the presence of noisy signals.

iii) We leverage the effectiveness of using the Mel Frequency Cepstral Coefficients (MFCCs), a widely used representation in voice recognition, for learning the probabilistic distribution of the seismic signals, enhancing the overall performance of our system.

The paper is organized as follows: Section II offers a brief overview of the related works in the field, Section III elaborates on the methodology with a focus on adapting the proposed system to seismic signals, Section III-E describes the hyperparameter optimization of A-MAD, Section IV presents the obtained results, and Section V concludes the study.

II. RELATED WORKS

Several studies have investigated the detection of volcano microseismic events using various techniques, including hidden Markov models (HMM), VAD, deep learning models, and other signal processing techniques.

HMM models were proposed by Gutiérrez et al. [10] for automatic microseismic event detection and classification. They applied their method to seismic data from the San Cristobal volcano in Nicaragua and achieved correct classification rates of up to 80%. Their results demonstrated the effectiveness of the HMM method in real-time detection, isolation, and identification of microseismic events. Similarly, Bhatti et al. [11] developed an automatic volcano event detection system based on HMMs that incorporated state and event duration models. They incorporated duration modeling to reduce false positive rates in event detection, resulting in high accuracy and a reduction of up to 31% in false positives.

Inspired by the speech processing community, Lara-Cueva et al. [12] proposed a real-time microseismic event detection system based on VAD techniques. They utilized VAD algorithms to detect long-period (LP) and volcano-tectonic (VT) events and determine their starting and ending points. Their algorithm achieved high accuracy with low

computational complexity, making it suitable for real-time volcanic research. Similarly, in [6], they aimed to enhance micro-earthquake detection using real-time automatic recognition systems based on VAD and endpoint detection. They developed a reliable detector with high precision, accuracy, and a low Balanced Error Rate (BER) using continuous data from the Cotopaxi Volcano in Ecuador.

Deep learning models have also been proposed by Titos et al. [13], where they utilized Recurrent Neural Networks (RNN), Long Short-Term Memory (LSTM), and Gated Recurrent Unit (GRU) for the detection and classification of continuous volcano-seismic events. They trained their models using a representative dataset and achieved high accuracy in detecting and classifying different types of events, showcasing the potential of RNNs for the real-time monitoring of volcanic activity. In addition, Lara et al. [14] have contributed to the field with an automatic recognition system for volcanic microearthquakes, with a particular focus on the Cotopaxi Volcano. Their approach leverages Convolutional Neural Networks (CNNs) and spectrograms generated using various window types based on the theory of periodograms. This approach exhibits remarkable performance with 99% accuracy in the detection stage and 97% accuracy in the classification stage.

Additionally, other signal processing techniques have been proposed in the literature. Specifically, Proaño et al. [15] investigated the use of Variational Mode Decomposition (VMD) for seismic event detection. They applied VMD to seismic signals from the Cotopaxi Volcano in Ecuador and found that it improved event detection and identification of event starting and ending points, reporting a 99.26% detection accuracy. Recently, a micro-earthquake detector based on homomorphic deconvolution and the STA/LTA algorithm was proposed [16]. The detector was applied to seismic data from the Cotopaxi volcano, achieving a 98.26% detection accuracy. According to the authors, the homomorphic deconvolution technique improved the estimation of the volcanic micro-earthquake signal while reducing signal noise. Table 1 summarizes the key aspects of the aforementioned related works.

Unlike previous works, our A-MAD approach extracts characteristics from each individual utterance, enabling adaptability to varying noise levels in different seismic signals. This adaptability sets our method apart from traditional approaches that rely solely on an energy threshold. Moreover, our system incorporates a spectral subtraction stage, which effectively enhances the SNR in seismic signals. This spectral subtraction technique enables robust detection even in the presence of noisy signals, addressing a common challenge faced in volcano microseismic event detection. Finally, inspired by the speech processing community, we utilize MFCCs as a representation.

III. METHODOLOGY

The proposed methodology, referred to as A-MAD, comprises two main stages: training and inference, as illustrated in Figure 1. Moreover, the subsections presented below are shown in the colored boxes of Figure 1. Initially, the original seismic signals, which inherently contain noise, are utilized to extract MFCCs for each time frame. Additionally, to enhance the signal quality and improve the SNR, a spectral subtraction technique is applied to these noisy signals as a preprocessing step. Subsequently, the energy of the enhanced seismic signal is computed and sorted in ascending order. Next, the MFCCs corresponding to the frames with the lowest and highest energy levels in the enhanced signal are selected and used to train two GMMs: one for identifying frames containing seismic events and the other for recognizing frames without seismic activity. Each MFCC frame is assigned a category based on the GMM classifications. Then, a decision algorithm, based on specific assumptions related to microseismic events, determines the start and end times of the detected microseismic events. Finally, performance metrics are computed by comparing the timestamps generated by A-MAD with the ground truth timestamps established by domain experts. Detailed explanations of each stage of the proposed methodology will follow in the subsequent sections.

A. DATASETS

A-MAD was applied to two distinct datasets of seismic signals collected from the Cotopaxi volcano. The first dataset, known as MicSigV1 [17], was obtained from the first publicly available repository of Ecuadorian volcano microseismic events, accessible at https://www.igepn.edu.ec/eseismic_web_site/. This dataset contains only discrete microseismic events. The second dataset, referred to as ConSig in this study, was specifically provided by the IGEPN for the purpose of this research. In contrast to MicSigV1, ConSig contains continuous data measurements.

The seismic signals were recorded by two broadband seismic stations, BREF and BVC2, with a sampling rate of 50 Hz, as well as a short-period seismic station, VC1, with a 100 Hz sampling rate. These stations are situated on the flanks of the Cotopaxi volcano. Both datasets encompass various types of seismic events, including LP, VT, regional, hybrid, and ice-quakes. Expert annotators from the IGEPN provided annotations for the signals, indicating the start and end times (timestamps) of each seismic event and its corresponding type. The seismic signals are stored in accordance with the Standard Exchange of Earthquake Data format (SEED) [18], which includes both the data and metadata for each file.

The MicSigV1 dataset consists of 1187 utterances, with each utterance capturing a single seismic event. Each utterance includes 10 s of the signal before and after the detected event, enabling the estimation of the noise level. The signals in this dataset originate from the BREF and VC1 stations. In contrast, the ConSig dataset spans a duration of 72 hours of continuous data and is segmented into 20-minute windows, as described in [6]. These windows may contain multiple seismic events or no events at all. IGEPN specialists have annotated a total of 77 seismic events recorded by the three seismic stations (BREF, BVC2, VC1).

TABLE 1. Summary of related works.

Study	Technique	Volcano	Dataset	Performance
[10]	Hidden Markov Models	San Cristobal (Nicaragua)	1098 seismic events from 600 hours of continuos data	Up to 80% accuracy
[11]	Hidden Markov Models	Llaima (Chile)	300 signals of 20 minutes each (total of 100 hours)	Up to 31% reduction in false positives 94% accuracy
[12]	Voice Activiy Detection	Cotopaxi (Ecuador)	436 seismiec events	95.2% accuracy Balanced Error Rate of 0.05%
[6]	Voice Activity Detection	Cotopaxi (Ecuador)	744 hours of continous data	97.89% precision 97.10% accuracy 0.15% of Balanced Error Rate
[13]	Recurrent Neural Networks	Deception Island (Antarctica)	512 continous streams containing 2193 events	Up to 94% of correctly detected and classified seismic events
[14]	Convolutional Neural Networks	Cotopaxi (Ecuador)	1187 seismic events	99% accuracy (detection) 97% accuracy (classification)
[15]	Variational Mode Decomposition	Cotopaxi (Ecuador)	436 seismic events	99.26% detection accuracy
[16]	Homomorphic deconvolution	Cotopaxi (Ecuador)	1187 seismic events	98.29% detection accuracy

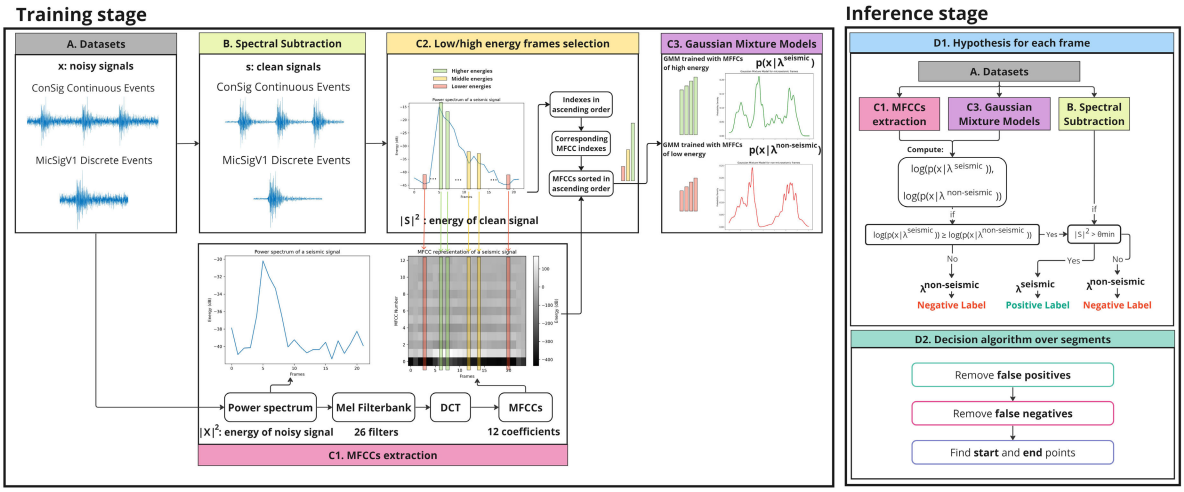

FIGURE 1. Flowchart of the adaptive-microseismic activity detector (A-MAD). During training, spectral subtraction, MFCCs extraction, and low/high energy frames selection are used to train two gaussian mixture models. For inference, a single label is predicted as a hypothesis for each input frame. Finally, false positives and false negatives are removed from all segments in the utterance, and the start and end points are defined.

In this context, the term 'utterance' refers to the entire seismic signal being analyzed. In the case of the MicSigV1 dataset, an utterance corresponds to one of the 1187 seismic signals containing a single microseismic event. In the case of the ConSig dataset, an utterance represents a 20-minute segment that may contain multiple microseismic events.

B. PREPROCESSING STAGE: SPECTRAL SUBTRACTION

The spectral subtraction technique is employed to enhance the quality of the seismic signal by reducing the background noise present in its spectrum. Let $|X|^2$ and $|N|^2$ represent the powers of the noisy original signal and its estimated noise, respectively, in a specific frequency FFT bin. The spectral subtraction process involves multiplying the noisy signal by a gain factor g, where g is defined for each frequency bin as [19]:

$$g = \max\left(\left(1 - \left(\alpha \frac{|N|^2}{|X|^2}\right)\right), \min\left(g_h, \left(\beta \frac{|N|^2}{|X|^2}\right)\right)\right). \quad (1)$$

Here, $g_h = 1$ denotes the maximum gain for the noise floor, $\beta = 0.01$ controls the maximum attenuation of noise in the power domain, and α denotes the over-subtraction factor. The value of α linearly decreases from $\alpha_{\max} = 10$ to $\alpha = 1$ according to the SNR as suggested in [20]. The Minimum Mean Square Error (MMSE) method serves as the noise estimator. The actual spectral weighting is then carried out by multiplying the noisy spectrum X with the weighting function g, resulting in the enhanced signal S in the frequency domain, defined as $S = g \cdot X$.

We used the VoiceBox toolbox implementation available at `specsub`[1] for the spectral subtraction stage, which provides the enhanced signal in the time domain. Finally, the energy of the enhanced signal is computed and proceeds to the subsequent stage.

C. MODELING THE DETECTION OF SEISMIC EVENTS

The modeling stage consists of three processes, which are explained separately: MFCCs extraction, low/high energy frames selection, and training of the GMMs.

[1] https://github.com/ImperialCollegeLondon/sap-voicebox

1) MFCCS EXTRACTION

The Mel scale is a perceptual pitch scale that approximates the frequency perception of the human auditory system. It is a non-linear scale based on the observation that the perception of pitch is not directly proportional to the physical frequency of a sound wave. Instead, the human ear perceives pitch differences on a logarithmic scale, as described in [21]. In this study, we employ a Mel scale filterbank consisting of 26 filters to reduce the number of frequency bins in the power spectrum of the seismic signal. This reduction helps to group together perceptually similar frequency components and focus on important spectral characteristics, while also reducing computational complexity.

The Mel filterbank spectrum was adjusted to accommodate the characteristics of volcanic seismic events, which predominantly manifest in low frequencies. Specifically, to incorporate this prior knowledge, in this paper, we considered the frequency range from 0 Hz to 50 Hz and assigned greater importance to the lower frequencies on the Mel scale.

After passing the power spectrum of the noisy seismic signal $|X|^2$ through the Mel filterbank, the logarithm of the filterbank outputs is subjected to the Discrete Cosine Transform (DCT) to decorrelate the filterbank coefficients and extract a compact representation of the spectral information [22]. The computation of MFCCs follows the equation:

$$\text{MFCC}_i = \sum_{k=1}^{26} X_k \cos\left[i\left(k-\frac{1}{2}\right)\frac{\pi}{26}\right],\ i = 1, 2, \ldots, M, \tag{2}$$

where $M = 12$ is the number of cepstrum coefficients, and X_k, for $k = 1, 2, \ldots, 26$ represents the log-energy output of the kth filter. This process allows us to obtain a compact representation of the spectral information that is relevant for the subsequent stages of the system.

2) LOW/HIGH ENERGY FRAMES SELECTION

In this stage, we compute the energy of the enhanced seismic signal $|S|^2$ obtained through the spectral subtraction stage. The energies are then sorted in ascending order while preserving the frame indexes. Since the number of frames in the frequency domain is consistent for the MFCCs and the energies computed in this step, we can establish a correspondence between these features.

To model the distributions of the presence or absence of a microseismic event based on the MFCCs, we divide the frames of each utterance into two sets. The first set consists of a fixed percentage of frames with the highest energies, which are used to train a GMM model representing the distribution of the presence of a microseismic event. The second set comprises a fixed percentage of frames with the lowest energies and is used to train a separate GMM model representing the distribution of the absence of a microseismic event. It is important to note that the percentage of frames for training both models (i.e., the percentage of training frames) is a hyperparameter in our A-MAD approach.

3) GAUSSIAN MIXTURE MODELS

As discussed in Bishop's book [23], GMMs are a statistical modeling technique used to handle complex data distributions that cannot be adequately represented by a single Gaussian distribution. In GMMs, the probability distribution of a dataset is represented as a weighted sum of K Gaussian components, each characterized by a mean vector $\boldsymbol{\mu}_k$ and a covariance matrix $\boldsymbol{\Sigma}_k$ for $k = 1$ to K. The mixing weights $\boldsymbol{\pi} = [\pi_1, \pi_2, \ldots \pi_K]$ assigned to each component indicate their relative importance in the mixture.

In our work, we adapt the methodology presented in [19] to the seismic domain. Specifically, we train two GMMs: one to represent frames containing microseismic events and another for frames without microseismic activity.

Our assumption is that frames with higher energy are indicative of microseismic activity, and we utilize them to define the GMM for microseismic events. Conversely, frames with lower energy are used to define the GMM for non-microseismic activity.

To reduce the computational complexity of our adaptive system, we employ the k-means algorithm instead of the Expectation-Maximization (EM) algorithm to estimate the GMM parameters. K-means can be viewed as a limit case of the EM algorithm in which the covariance matrices of the GMMs are assumed to be identical and spherical. The k-means algorithm assigns each MFCC vector to the nearest cluster centroid based on Euclidean distance, and the centroids are updated by calculating the mean of the assigned data points. We use $K = 16$ Gaussian components for both GMM models, whose means correspond to the cluster centroids obtained from k-means. The k-means algorithm iterates a maximum of 20 epochs to refine the clustering results. The learned microseismic and non-microseismic event models are GMMs of the form:

$$p(\boldsymbol{x}|\lambda) = \sum_{k=1}^{K} \pi_k \mathcal{N}(\boldsymbol{x}|\boldsymbol{\mu}_k, \boldsymbol{\Sigma}_k), \tag{3}$$

where $\boldsymbol{\pi}$ are the mixing weights, $\boldsymbol{\mu}_k$ the mean vectors, $\boldsymbol{\Sigma}_k$ the covariance matrices, $\boldsymbol{x}$ the MFCC vector of an arbitrary frame within the utterance and λ refers to one of the two trained GMM models. Specifically, we use λ^{seismic} to represent the microseismic activity hypothesis and $\lambda^{\text{non-seismic}}$ to represent the non-microseismic activity hypothesis. This formulation will be utilized during the inference stage.

D. INFERENCE AND DECISION ALGORITHM

Once defined the parameters of the GMMs, we compute the Log-Likelihood Ratio (LLR) of every utterance frame for the given models, followed by a decision algorithm. Later in this document, we will provide a detailed explanation of the metrics used to evaluate our approach.

1) HYPOTHESIS FOR EACH FRAME

The A-MAD algorithm utilizes the LLR test to compare the likelihoods of the microseismic activity hypothesis (λ^{seismic})

and the non-microseismic activity hypothesis ($\lambda^{\text{non-seismic}}$) for each frame. Assuming equal priors for microseismic and non-microseismic activity, the LLR test for the presence of microseismic activity in a given frame $\boldsymbol{x}$ within an utterance is defined as:

$$\log\left(p(\boldsymbol{x}|\lambda^{\text{seismic}})\right) \geq \log\left(p(\boldsymbol{x}|\lambda^{\text{non-seismic}})\right), \quad (4)$$

where $p(\boldsymbol{x}|\lambda)$ is calculated using Eq. 3 based on the corresponding hypothesis.

Similar to the speech activity case discussed by [19], the condition to declare the presence of microseismic activity for a specific frame $\boldsymbol{x}$ is reduced from Eq. 4 to the nearest neighbor rule:

$$\min_k ||\boldsymbol{x} - \boldsymbol{\mu}_k^{\text{seismic}}||^2 \leq \min_k ||\boldsymbol{x} - \boldsymbol{\mu}_k^{\text{non-seismic}}||^2, \quad (5)$$

where $\boldsymbol{\mu}_k^{\text{seismic}}$ and $\boldsymbol{\mu}_k^{\text{non-seismic}}$ represent the mean vectors learned by the GMMs for the microseismic activity hypothesis (λ^{seismic}) and the non-microseismic activity hypothesis ($\lambda^{\text{non-seismic}}$), respectively. It is important to highlight that in our methodology, the minimum distance to centroids, as represented in Eq. 5, and the LLR test, as shown in Eq. 4, are essentially equivalent. In the LLR test, we evaluate the likelihood of a given data point, denoted as $\boldsymbol{x}$, under the microseismic activity hypothesis compared to the likelihood under the non-microseismic activity hypothesis. Conversely, when we select the centroid (Gaussian component) with the minimum distance, we are effectively choosing the class that data point $\boldsymbol{x}$ is most similar (i.e., close) to. This mirrors the concept of selecting the hypothesis (or class) that renders data point $\boldsymbol{x}$ more probable in the LLR test.

Finally, to classify a frame as containing microseismic activity, it must satisfy the LLR condition described in Eq. 5, and the frame's energy must surpass a minimum energy threshold θ_{min}, which is a hyperparameter of the A-MAD algorithm.

2) DECISION ALGORITHM

From the previous stage, we obtain frames that are labeled as either having microseismic activity (positive label) or non-microseismic activity (negative label). These labeled frames are then grouped into segments, where a segment consists of consecutive frames with the same label, either positive (microseismic activity) or negative (non-microseismic activity).

The decision algorithm is utilized to determine the start and endpoint of the detected events within an entire utterance. Considering the reported average duration of seismic events in the Cotopaxi volcano, as mentioned in [24] and [6] to be approximately20 s, the decision algorithm aims to mitigate potential false positive (FP) and false negative (FN) segments.

FP segments arise from short-duration energy peaks that cannot be attributed to a seismic event. Specifically, positive segments shorter than 4 s, which are surrounded by frames labeled as negative, are reclassified as negative segments.

Afterward, a similar process is applied to address FN segments. Concretely, negative segments shorter than 4 s, surrounded by frames labeled as positive, are reclassified as positive segments.

Next, the decision algorithm identifies positive segments that are at least 8 s long, which are considered to likely contain seismic activity.

Finally, the start and end times in seconds are computed based on the frame numbers from all positive segments found. This conversion allows for the comparison of the timestamps estimated by the A-MAD with the ground truth labels provided by experts from the IGEPN.

3) METRICS

As mentioned in [17], the evaluation of volcanic 4 s event detectors relies on two performance metrics: accuracy (Acc) and BER. The accuracy metric measures the proportion of correctly detected events out of the total number of events. On the other hand, the BER value ranges from 0 to 1, with an optimal value of 0 indicating perfect performance. The IGEPN requires a BER not greater than 0.01 for the detection of volcanic microseismic events at the Cotopaxi volcano. These metrics are computed based on the number of true positives (TP), true negatives (TN), false positives (FP), and false negatives (FN), defined as follows:

$$Acc(\%) = \frac{TP}{TP + TN} \times 100 \quad (6)$$

$$BER = 1 - \frac{\frac{TP}{TP+FN} + \frac{TN}{TN+FP}}{2} \quad (7)$$

In this context, a volcanic seismic event is considered a TP if the difference between the true and estimated timestamps is less than 5 s. FN occurs when the estimated timestamps exceed the true event duration by more than 5 s, while FP happens if the estimated timestamps start or end more than 5 s before or after the true event. These metrics will be computed for both datasets to evaluate the performance of the proposed approach.

E. HYPERPARAMETER OPTIMIZATION

We performed three experiments to optimize the hyperparameters of the A-MAD system: the window length, the percentage of training frames for the GMM models, and the minimum energy threshold θ_{min}. The window length needs to be modified because of the differences in sampling frequencies between audio signals and seismic signals recorded by the Cotopaxi volcano's sensors. s for the percentage of training frames, we varied the samples from 10% to 50% with the aim of determining the GMM parameters that yield the best metrics. Finally, for the experiments of the minimum energy threshold, we used the optimal window length and the optimal percentage of training frames, since this parameter is crucial in distinguishing frames with and without activity. The optimization experiments will be presented in Section IV-A.

TABLE 2. Optimization of the window length on the MicSigV1 and ConSig datasets.

Window size $[s]$	Overlapping $[s]$	ConSig Acc (%)	MicSigV1 Acc (%)
0.03	0.01	81.27	77.45
0.5	0.25	84.26	90.67
1	0.5	97.12	91.43
1.5	0.75	97.43	92.89
2	**1**	**98.45**	**96.68**
3	1.5	95.37	90.44
5	2.5	90.26	86.15
10	5	87.16	43.26

IV. RESULTS

This section describes the results for the experimental setup performed for hyperparameter optimization of the A-MAD system. Then, the MicSigV1 and ConSig datasets are used to assess the performance of our system.

A. EXPERIMENTAL SETUP

The A-MAD algorithm was implemented using Matlab® on a computer equipped with an Intel Core i7 processor running at 2.40 GHz and 8 GB of RAM. No graphical processing unit (GPU) acceleration was utilized.

1) WINDOW LENGTH

The need to modify this parameter arises from the differences in sampling frequencies between audio signals (16 kHz - 48 kHz) and seismic signals recorded by the Cotopaxi volcano's sensors (50 Hz or 100 Hz). Seismic signals have significantly lower sampling rates, resulting in fewer samples per second. In speech signals, a window length of 0.03 s with 0.01 s of overlapping was suggested by [19]. However, for seismic signals, [6] used a window size of 0.1 s with 50% of overlapping. In our experiments, we tested different window sizes as listed in Table 2, and we found that using a window size of 2 s with 50% of overlapping yielded the highest accuracy for both datasets.

2) PERCENTAGE OF TRAINING FRAMES

According to [19], using 10% of the frames with the lowest and highest energies is the best approach for training the GMMs for speech signals. However, we observed that slightly increasing the percentage of frames used to train the GMMs can improve the A-MAD performance. Therefore, we conducted experiments with different percentages of frames, as shown in Table 3. Our findings indicate that using 30% of frames with the lowest and highest energies is the most suitable choice for our A-MAD.

This percentage provides an adequate number of data samples to model the distributions for detecting volcanic microseismic events. Conversely, using more than 30% of frames reduces the models' generalization capacity.

3) MINIMUM ENERGY THRESHOLD

Once the optimal window length and the appropriate percentage of training frames have been determined, the selection of the minimum energy threshold becomes crucial in distinguishing frames with and without activity. It is worth noting that in traditional VAD systems, the minimum energy threshold is often the only parameter adjusted. However, in our A-MAD, this parameter is examined alongside the LLR hypothesis for frame classification.

TABLE 3. Optimization of the percentage of training frames on the MicSigV1 and ConSig datasets.

Training frames (%)	ConSig Acc (%)	MicSigV1 Acc (%)
10	96.12	92.39
20	97.67	93.25
30	**98.45**	**96.68**
40	91.26	93.09
50	89.55	92.52

TABLE 4. Optimization of the minimum energy threshold on the MicSigV1 and ConSig datasets.

Min Energy $\theta_{min}[dB]$	ConSig Acc (%)	MicSigV1 Acc (%)
-17	91.26	84.16
-19	96.25	91.16
-20	**98.45**	**96.68**
-22	98.17	92.51
-24	97.27	92.52
-28	97.17	92.46

To determine the minimum energy threshold, we analyzed the energy values of the lowest 30% frames in each utterance of the MicSigV1 dataset. We identified the maximum and minimum energy values, calculating the average of these values to establish an estimated range for the minimum energy threshold. The average minimum energy value was -32.59 dB, while the average maximum energy value was -14.67 dB. Subsequently, we evaluated the performance of the A-MAD by varying θ_{min} within the specified range, as depicted in Table 4. We observed that our system achieved optimal performance when θ_{min} was set to -20 dB.

These modifications allow for precise parameter selection in the A-MAD, enhancing its performance and effectiveness in detecting microseismic events. In the following section, we present the metrics obtained using the optimized hyperparameters.

B. A-MAD SYSTEM EVALUATION

For the MicSigV1 dataset, we focused on signals recorded by the BREF station. As for the ConSig dataset, signals from three stations were utilized: BREF, BVC2, and VC1. The decision algorithm employed for the MicSigV1 dataset followed the description provided in Section III-D2, where a threshold of 5 s was validated to classify an event as a TP (see Figure 2 for an illustration).

In contrast, an additional decision step was required for the ConSig dataset due to the involvement of three seismic signals (i.e., from the BREF, BVC2, and VC1 stations). Following the guidance of experts from the IGEPN, we established that a volcanic microseismic event would be considered detected if it was correctly identified in at least two out of the three stations.

Figure 3 illustrates an example that demonstrates the decision process for the ConSig dataset. In the case of the first event, it was correctly classified as a true positive because it was detected by both the BREF and BVC2 stations within the

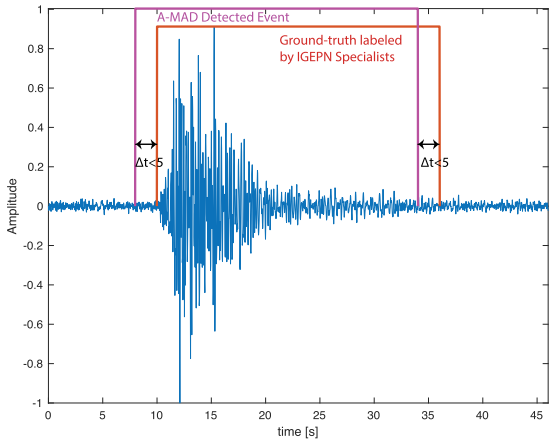

FIGURE 2. A volcanic microseismic event from MicSigV1 is considered a true positive (TP) if the difference between the ground-truth labeled by IGEPN specialists and the estimated timestamps of our A-MAD approach are less than 5 s.

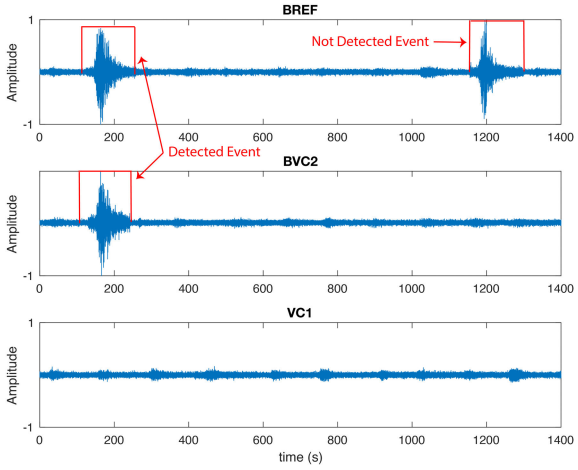

FIGURE 3. Decision algorithm for the consig dataset. The event on the left is considered detected as it was correctly identified in at least two out of three stations (BREF and BVC2) within the specified 5-second threshold. However, the event on the right is not considered detected as it was only identified by the BREF station and not in the other stations.

specified 5 s threshold. However, for the second event, it was only detected by the BREF station and therefore was not considered a TP. By incorporating these decisions, we were able to evaluate the performance of the A-MAD algorithm on both datasets, providing valuable insights into its accuracy and BER in detecting volcanic microseismic events.

We compared our results with the detection task conducted in [14], where each utterance from the MicSigV1 dataset was segmented into 15 s windows, and a decision was made for each segment. Therefore, the segmentation approach employed by [14] can be compared to our A-MAD threshold of 5 s. However, our method is more stringent, as it penalizes differences in timestamps greater than 5 s. Our evaluation metrics for the MicSigV1 dataset demonstrated competitive accuracy and BER values, as presented in Table 4. Notably, we achieved a BER of 0.012, meeting the performance requirement set by the IGEPN for the detection of volcanic microseismic events at the Cotopaxi volcano.

Additionally, we achieved a higher performance for the ConSig dataset than for the MicSigV1 dataset, with an accuracy of 98.45 %. This improvement can be attributed to the characteristics of the ConSig dataset, which consists of utterances containing 20 min of volcano seismic signal. The use of 30 % of frames for modeling the microseismic and non-microseismic models provides more contextual information, resulting in more robust models compared to the MicSigV1 dataset, where only 10 s before and after the volcanic seismic event are included.

Furthermore, we compare our approach for continuous seismic signals from the Cotopaxi volcano with three related works. First, the ConSig MDA [6] approach is similar to ours since the continuous signals were segmented in 20 min, and more than one micro-earthquake can be present in the segment or no events at all. Even though the dataset used in [6] contains 744 h of seismic signals, it can still be compared with our system, which achieved [6] 1.35% higher accuracy than ConSig MDA. Second, we compare our system with the approach for detecting micro-seismic events proposed in [16],

TABLE 5. A-MAD performance evaluation on the ConSig and MicSigV1 datasets. We compare our results with similar approaches presented in [6], [14], [25], and [16].

System	Acc (%)	BER
MicSigV1 A-MAD	**96.39**	**0.012**
MicSigV1 [14]	95.50	0.07
ConSig A-MAD	**98.45**	**0.011**
ConSig MDA [6]	97.10	0.015
ConSig Deconv [16]	98.29	**0.011**
ConSig ANN [25]	0.011	0.015

which used homomorphic deconvolutions to improve the SNR, followed by a STA/LTA detector. The system referred to as ConSig Deconv [16] was evaluated on continuous seismic signals from the Cotopaxi volcano as well, reaching a high accuracy proportional to our results. Lastly, the ConSig ANN [25] system trained machine learning classifiers along with diverse labeling techniques to achieve an accuracy of 95.4% for continuous seismic signals of the Cotopaxi volcano. Table 4 presents the comparative results of evaluating the microseismic detectors with continuous seismic signals. Note that the accuracy was improved with our A-MAD system, and the BER required by the IGEPN was satisfied.

Based on the observed results, we hypothesize that the MicSigV1 dataset is more suitable for the classification of volcanic microseismic events, while a continuous seismic signal with greater duration and multiple events, such as the ConSig dataset, can lead to the development of more robust models for detection purposes. A similar behavior was observed in [14], where the probability of detection increased for signals with a duration longer than 30 s.

Another aspect in which we can compare our A-MAD system is the execution time. According to the authors of [14], their system requires approximately 0.65 s to 0.75 s to process a window of 15 s. In contrast, our A-MAD is capable of processing an entire MicSigV1 utterance (approximately 1 min in duration) in just 0.34 s. For the ConSig dataset, our A-MAD takes 5.57 s to process and detect events in a 20-minute signal, whereas the approach presented in [14]

requires 55 s to detect and classify a signal of the same duration, while the approach of [6] processes a signal of the same duration in 2.04 s.

One notable advantage of our system is its efficiency and speed, as it does not rely on the use of a GPU to accelerate the training process. Deep learning approaches, such as the one presented in [14], depend on pre-trained models that may require several hours or even days to complete the training process without sufficient computational resources. This demonstrates the efficiency and computational speed of our A-MAD system, making it suitable for real-time microseismic event detection applications. In contrast, we acknowledge that the deep learning architecture presented in [14] successfully accomplishes both the detection and classification tasks.

V. CONCLUSION

This work contributes to the advancement of early warning systems for volcanic eruptions, with a particular focus on the Cotopaxi volcano. However, the methodology proposed for the A-MAD system can be extended to analyze volcanic signals from different volcanoes, making it a versatile approach. Our system involves a preprocessing stage, where the energy signal is enhanced using spectral subtraction. This is followed by a modeling stage, where Gaussian Mixture Models are trained using the MFCCs of frames with the lowest and highest energies. These models aim to capture the distributions that represent the presence of microseismic or non-microseismic volcanic activity. Once the model parameters are learned, a decision is generated for each frame based on the log-likelihood ratio of the energy frame and the centroids of the models, along with a minimum energy threshold that was determined experimentally.

The results obtained demonstrate the effectiveness of our A-MAD system as a real-time detector of volcanic microseismic events. In the MicSigV1 dataset, which consists of discrete events, our system achieved an accuracy of 96.39 % and 0.012 of BER. Similarly, in the ConSig dataset, which contains continuous seismic signals, our system achieved an accuracy of 98.45 % with 0.011 of BER. The performance metrics attained, along with the efficient execution time of our A-MAD system, align with the requirements specified by the IGEPN, which is the institution responsible for monitoring volcanic activity in Ecuador.

Future work might investigate the integration of other data modalities, such as infrasound or gas emission data, in conjunction with seismic signals. Combining multiple data sources can provide a more comprehensive understanding of volcanic activity and improve the detection of volcanic events.

ACKNOWLEDGMENT

The authors would like to express their sincere gratitude to Instituto Geofísico de la Escuela Politécnica Nacional (IGEPN) for providing the datasets used in this research and for their valuable assistance and guidance throughout the project. They also express their special appreciation to Mario Ruiz, Volcanologist and the Head of IGEPN, for his expertise and invaluable support in this work. Special thanks to the SRASI Project of Universidad de las Fuerzas Armadas—ESPE, which aims to implement a system for automatic detection of seismic signals of the Cotopaxi volcano.

REFERENCES

[1] S. R. McNutt, "Volcanic seismology," *Annu. Rev. Earth Planet. Sci.*, vol. 32, pp. 461–491, Feb. 2005.

[2] B. A. Chouet, R. A. Page, C. D. Stephens, J. C. Lahr, and J. A. Power, "Precursory swarms of long-period events at Redoubt Volcano (1989–1990), Alaska: Their origin and use as a forecasting tool," *J. Volcanol. Geothermal Res.*, vol. 62, nos. 1–4, pp. 95–135, Aug. 1994.

[3] B. A. Chouet, "Long-period volcano seismicity: Its source and use in eruption forecasting," *Nature*, vol. 380, no. 6572, pp. 309–316, Mar. 1996.

[4] D. M. Pyle, T. A. Mather, and J. Biggs, "Remote sensing of volcanoes and volcanic processes: Integrating observation and modelling–introduction," *Geol. Soc., London, Special Publications*, vol. 380, no. 1, pp. 1–13, 2013.

[5] F. Rodriguez, T. Toulkeridis, W. Sandoval, O. Padilla, and F. Mato, "Economic risk assessment of cotopaxi volcano, ecuador, in case of a future lahar emplacement," *Natural Hazards*, vol. 85, no. 1, pp. 605–618, Jan. 2017.

[6] R. Lara, M. Rodriguez, and J. Larco, "A real-time microearthquakes-detector based on voice activity detection and endpoint detection: An approach to cotopaxi volcano," *J. Volcanol. Geothermal Res.*, vol. 400, Aug. 2020, Art. no. 106867.

[7] F. Grijalva, W. Ramos, N. Pérez, D. Benítez, R. Lara-Cueva, and M. Ruiz, "ESeismic-GAN: A generative model for seismic events from cotopaxi volcano," *IEEE J. Sel. Topics Appl. Earth Observ. Remote Sens.*, vol. 14, pp. 7111–7120, 2021.

[8] P. S. Earle and P. M. Shearer, "Characterization of global seismograms using an automatic-picking algorithm," *Bull. Seismol. Soc. Amer.*, vol. 84, no. 2, pp. 366–376, Apr. 1994.

[9] R. A. Lara-Cueva, D. S. Benítez, E. V. Carrera, M. Ruiz, and J. L. Rojo-Álvarez, "Feature selection of seismic waveforms for long period event detection at cotopaxi volcano," *J. Volcanol. Geothermal Res.*, vol. 316, pp. 34–49, Apr. 2016.

[10] L. Gutiérrez, J. Ibanez, G. Cortés, J. Ramírez, C. Benítez, V. Tenorio, and A. Isaac, "Volcano-seismic signal detection and classification processing using hidden Markov models. Application to San Cristóbal volcano, Nicaragua," in *Proc. IEEE Int. Geosci. Remote Sens. Symp.*, vol. 4, Jul. 2009, p. IV-522.

[11] S. M. Bhatti, M. S. Khan, J. Wuth, F. Huenupan, M. Curilem, L. Franco, and N. B. Yoma, "Automatic detection of volcano-seismic events by modeling state and event duration in hidden Markov models," *J. Volcanol. Geothermal Res.*, vol. 324, pp. 134–143, Sep. 2016.

[12] R. A. Lara-Cueva, A. S. Moreno, J. C. Larco, and D. S. Benítez, "Real-time seismic event detection using voice activity detection techniques," *IEEE J. Sel. Topics Appl. Earth Observ. Remote Sens.*, vol. 9, no. 12, pp. 5533–5542, Dec. 2016.

[13] M. Titos, A. Bueno, L. García, M. C. Benítez, and J. Ibañez, "Detection and classification of continuous volcano-seismic signals with recurrent neural networks," *IEEE Trans. Geosci. Remote Sens.*, vol. 57, no. 4, pp. 1936–1948, Apr. 2019.

[14] F. Lara, R. Lara-Cueva, J. C. Larco, E. V. Carrera, and R. León, "A deep learning approach for automatic recognition of seismo-volcanic events at the cotopaxi volcano," *J. Volcanol. Geothermal Res.*, vol. 409, Jan. 2021, Art. no. 107142.

[15] E. Proaño, D. S. Benítez, R. Lara-Cueva, and M. Ruiz, "On the use of variational mode decomposition for seismic event detection," in *Proc. IEEE Int. Autumn Meeting Power, Electron. Comput. (ROPEC)*, Nov. 2018, pp. 1–6.

[16] F. Lara, R. León, R. Lara-Cueva, A. F. Tinoco-S., and M. Ruiz, "Detection of volcanic microearthquakes based on homomorphic deconvolution and STA/LTA," *J. Volcanol. Geothermal Res.*, vol. 421, Jan. 2022, Art. no. 107439.

[17] N. Pérez, D. Benítez, F. Grijalva, R. Lara-Cueva, M. Ruiz, and J. Aguilar, "ESeismic: Towards an ecuadorian volcano seismic repository," *J. Volcanol. Geothermal Res.*, vol. 396, May 2020, Art. no. 106855.

[18] A. T. Ringler and J. R. Evans, "A quick SEED tutorial," *Seismol. Res. Lett.*, vol. 86, no. 6, pp. 1717–1725, Nov. 2015.
[19] T. Kinnunen and P. Rajan, "A practical, self-adaptive voice activity detector for speaker verification with noisy telephone and microphone data," in *Proc. IEEE Int. Conf. Acoust., Speech Signal Process.*, May 2013, pp. 7229–7233.
[20] T. Gerkmann and R. C. Hendriks, "Unbiased MMSE-based noise power estimation with low complexity and low tracking delay," *IEEE Trans. Audio, Speech, Language Process.*, vol. 20, no. 4, pp. 1383–1393, May 2012.
[21] J. Volkmann, S. S. Stevens, and E. B. Newman, "A scale for the measurement of the psychological magnitude pitch," *J. Acoust. Soc. Amer.*, vol. 8, no. 3, p. 208, Jan. 1937.
[22] S. Davis and P. Mermelstein, "Comparison of parametric representations for monosyllabic word recognition in continuously spoken sentences," *IEEE Trans. Acoust., Speech, Signal Process.*, vol. ASSP-28, no. 4, pp. 357–366, Aug. 1980.
[23] C. M. Bishop and N. M. Nasrabadi, *Pattern Recognition and Machine Learning*, vol. 4, no. 4. New York, NY, USA: Springer, 2006.
[24] D. Andrade, M. Hall, P. Mothes, L. P. T. Salgado, J.-P. Eissen, P. Samaniego, J. Egred, P. Ramón, D. Rivero, and H. Yepes, *Los Peligros Volcánicos Asociados con el Cotopaxi*. Quito, Ecuador: Corporación Editora Nacional, CEN/Escuela Politécnica Nacional, 2005.
[25] E. V. Carrera, A. Pérez, and R. Lara-Cueva, "Automated systems for detecting volcano-seismic events using different labeling techniques," in *Proc. 1st Int. Conf. Appl. Technol. (ICAT)*, Quito, Ecuador. Edinburgh, U.K.: Springer, 2020, pp. 133–144.

KAREN ROSERO (Graduate Student Member, IEEE) received the B.S. degree in electrical engineering and telecommunications from the Army Polytechnic School, Sangolquí, Ecuador, in 2020, and the M.Sc. degree in electrical engineering from the School of Electrical and Computer Engineering, University of Campinas (UNICAMP), Campinas, Brazil, in 2022. She is currently pursuing the Ph.D. degree with The University of Texas at Dallas. Her research interests include spatial audio, deep learning, music information retrieval, affective computing, and multimodal signal processing.

CARLA PARRA received the B.Sc. degree in information technology from Escuela Politécnica Nacional, Quito, Ecuador, in 2019, and the master's degree in business administration from the EAE Bussiness School, Barcelona, Spain, in 2020. She is currently pursuing the part-time Ph.D. degree with Rey Juan Carlos University (URJC), Madrid, Spain. She serves as the Chief Technical Officer for NuCom, Barcelona. Her research interests include machine learning and software-defined radio applications.

FELIPE GRIJALVA (Senior Member, IEEE) received the B.S. degree in electrical engineering and telecommunications from the Army Polytechnic School, Sangolquí, Ecuador, in 2010, and the M.Sc. and Ph.D. degrees in electrical engineering from the University of Campinas, Campinas, Brazil, in 2014 and 2018, respectively. He is currently an Assistant Professor with Universidad San Francisco de Quito, Ecuador. His research interests include signal processing, machine learning, and computer vision applications.

JULIO CÉSAR LARCO (Member, IEEE) received the electronics engineering degree from Escuela Politécnica del Ejército, in 1997, and the M.Sc. degree in electrical and computer engineering from Universidade Estadual de Campinas (UNICAMP), Campinas, Brazil, in 2005. He is currently a Professor with the Electric Electronic and Telecommunications Department, Universidad de las Fuerzas Armadas, Ecuador. His research interests include digital signal processing, pattern recognition, and assistive technologies aimed at visually impaired people.

ROMÁN LARA-CUEVA (Senior Member, IEEE) received the B.Eng. degree in electronic and telecommunications engineering from Escuela Politécnica Nacional, Quito, Ecuador, in 2001, the M.Sc. degree in wireless systems and related technologies from Politecnico di Torino, Turin, Italy, in 2005, and the M.Sc. and Ph.D. degrees in telecommunication networks for developing countries from Rey Juan Carlos University, Fuenlabrada, Spain, in 2010 and 2015, respectively. In 2002, he joined Departamento de Eléctrica, Electrónica y Telecomunicaciones, Universidad de las Fuerzas Armadas (ESPE), Sangolquí, Ecuador, where he has been an Associate Professor, since 2005, and a Full Professor, since 2016. He founded and heads the Ad Hoc Network Research Center (CIRAD) and the Smart Systems Research Group (WiCOM-Energy), ESPE. He has been an External Professor with King Juan Carlos University, Spain, since 2017. He has authored more than 50 refereed and conference papers on topics related to wireless communications, signal processing, and machine learning. He is the author or coauthor in 13 publicly funded research projects and directed eight of them. His current research interests include digital signal processing and machine learning theory applied to wireless communications systems, and volcano seismology, also in the scope of the Internet of Things by developing smart gadgets for smart cities. He received the Prize of Best Junior Researcher from ESPE, in 2014, and the Best Researcher from the IEEE Ecuador Section, in 2017. He has served as the Chair for the IEEE Communications Society Ecuador, from 2020 to 2021.

NATHALY OROZCO GARZÓN (Senior Member, IEEE) received the electronic and telecommunications engineering degree from Armed Forces University (ESPE), Ecuador, in 2011, and the M.Sc. and Ph.D. degrees in electrical engineering from the University of Campinas (UNICAMP), Brazil, in 2014 and 2018, respectively. She is currently an Assistant Professor with Universidad de Las Américas (UDLA), Quito, Ecuador. Her research interests include digital and wireless communications, computer applications, software simulation, MIMO, cognitive systems, machine learning, and 5G technologies. She received the HCIA-5G Certification from Huawei, in 2020.